1-2007

Uveal spindle cell tumor of blue-eyed dogs: an immunohistochemical study. Zarfoss M, Klauss G, Newkirk K, Kiupel M, Jones Y, Colitz C, Weisbrode S, Kusewitt D, Dubielzig R.

Kim M. Newkirk
University of Tennessee - Knoxville, knewkirk@utk.edu

Uveal Spindle Cell Tumor of Blue-Eyed Dogs: An Immunohistochemical Study

M. K. Zarfoss, G. Klauss, K. Newkirk, M. Kiupel, Y. Jones, C. M. H. Colitz and R. R. Dubielzig

Vet Pathol 2007 44: 276
DOI: 10.1354/vp.44-3-276

Vet Pathol **44**:276–284 (2007)

Uveal Spindle Cell Tumor of Blue-Eyed Dogs: An Immunohistochemical Study

M. K. Zarfoss, G. Klauss, K. Newkirk, M. Kiupel, Y. Jones, C. M. H. Colitz, and R. R. Dubielzig

Department of Pathobiological Sciences, University of Wisconsin-Madison, Madison, WI (MZ, RD); the University of Minnesota Veterinary Medical Center, St. Paul, MN (GK); The Ohio State University Department of Veterinary Biosciences, Columbus OH (KN, CC); and the Michigan State University Diagnostic Center for Population and Animal Health, Lansing, MI (MK, YJ)

Abstract. Immunohistochemical techniques were used to investigate the origin of a spindle cell tumor in the anterior uveal tract of dogs and the influence of ultraviolet radiation on the development of this tumor. Thirteen tumors were identified from the 4,007 canine ocular samples examined at the Comparative Ocular Pathology Laboratory of Wisconsin between 1978 and 2005. Siberian Husky and Siberian Husky mix dogs were overrepresented (10/13 dogs, overall median age 10 years). Light microscopic evaluation (all dogs) and electron microscopy (2 dogs) were performed. Immunohistochemical staining included alpha-smooth muscle actin (SMA), vimentin, S-100, desmin, glial fibrillary acidic protein (GFAP), Melan A, microphthalmic transcription factor (MITF-1), protein gene product 9.5 (PGP 9.5), laminin, gadd45, p53, proliferating cell nuclear antigen (PCNA), anti-UVssDNA (antibody for detection of (6-4)-dipyrimidine photoproducts), and telomerase reverse transcriptase (TERT). All tumors occurred in the iris with or without ciliary body involvement and were composed of spindle cells arranged in fascicles and whorls (variable Antoni A and B behavior). All tumors were positive when immunostained for vimentin and S-100. Nine of 13 tumors exhibited GFAP immunopositivity. All tumors were negative for SMA, desmin, Melan A, and MITF-1. Tumors were variably positive for PGP 9.5, laminin, gadd45, p53, PCNA, anti-UVssDNA, and TERT. Electron microscopy revealed intermittent basal laminae between cells. These tumors are morphologically and immunohistochemically most consistent with schwannoma. The relationship between spindle cell tumors of the anterior uvea of dogs, altered neural crest, blue iris color, and ultraviolet radiation has not yet been fully elucidated.

Key words: Canine; eye; immunohistochemistry; iris; neural crest; schwannomas; spindle; tumor.

Intraocular spindle cell tumors of dogs are rare and include melanocytic tumors,[11] peripheral nerve sheath tumors,[43] and metastatic sarcomas. The most common metastatic spindle cell tumors of the canine eye at the Comparative Ocular Pathology Laboratory of Wisconsin (COPLOW) are hemangiosarcoma, osteosarcoma, metastatic malignant melanoma, and anaplastic mesenchymal tumors of undetermined origin. At the COPLOW, a morphologically distinct spindle cell tumor has been identified that is exclusively associated with partial or complete blue uveal color.[28,29] The association between blue iridal color and tumors has been most extensively studied in humans in association with intraocular melanoma[20,30] and patients with neurocristopathies who exhibit both pigment abnormalities and peripheral nerve sheath tumors.[42] In blue eyes, there is virtually no histopathologically visible melanin within the iris stroma; it is present only in the posterior iridal epithelium. Melanin absorbs ultraviolet (UV) radiation;[2,22] UV radiation has been implicated in the pathogenesis of human uveal melanoma[2,22,44,46] and skin cancer.[39]

The purpose of this study was to describe a morphologically distinct uveal tumor of blue-eyed dogs and to perform immunohistochemical staining to investigate both the cell of origin and the cause of malignant transformation relative to (blue) uveal color. Immunohistochemical stains were used to rule out melanoma (Melan A, MITF-1), to rule in a tumor of peripheral nerve sheath origin (vimentin, S-100, glial fibrillary acidic protein [GFAP], protein gene product 9.5 [PGP 9.5], laminin), and to investigate the role of UV damage in the pathogenesis of this tumor (p53, anti-UVssDNA [antibody for detection of (6-4)-dipyrimidine photoproducts], proliferating cell nuclear antigen [PCNA], gadd45, and TERT).

Materials and Methods

Thirteen canine anterior uveal spindle cell tumors from the COPLOW collection were included in this

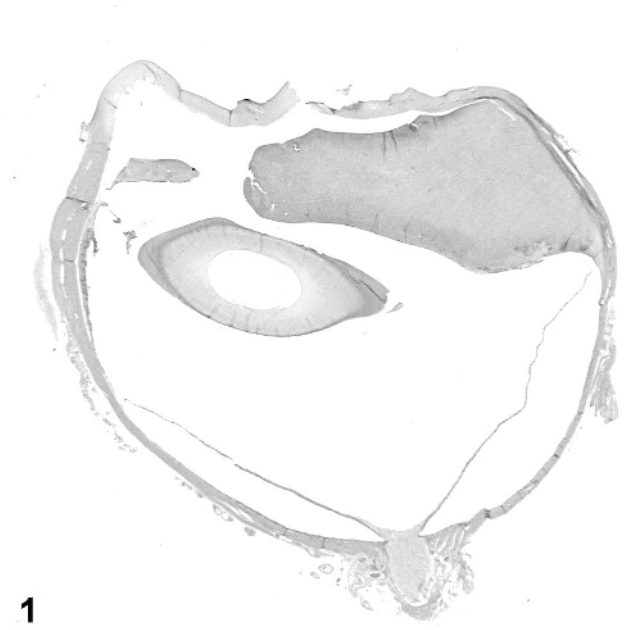

Fig. 1. Subgross photo of an eye (anterior at top, optic nerve at bottom); dog No. 13. The image shows an asymmetric expansion of the anterior uvea by spindle-cell tumor. Retinal detachment and corneal defects are artifactual. HE stain.

study based solely on their morphologic features. All tumors in this study involved the anterior uvea (Fig. 1) of blue-eyed dogs. All tissues were formalin fixed and paraffin embedded. All stains performed on the 13 tumors included are reported. Immunohistochemistry for these dogs was performed based on tissue availability. Immunohistochemical staining results are reported in Table 1 as follows: negative = < 10% of neoplastic cells stained positively; + = 10–25% positive; ++ = 25–50% positive; and +++ = > 50% positive.

The following stains were performed at the CO-PLOW: vimentin (Clone V9, No. M 0725, Dako Corp., Carpinteria, CA); GFAP (No. Z 0334, Dako); smooth muscle actin (Clone 1A4, No. M 0851, Dako); and desmin (Clone D33, No. M 0760, Dako). For these stains, 5-μm sections were mounted on slides and allowed to dry overnight at 56°C. Slides were placed in warm xylene, deparaffinized with 3 changes of xylene for 5 minutes each, and then hydrated in water. Samples were blocked for endogenous peroxidase with 3% H_2O_2 for 5 minutes. Samples were rinsed in distilled water before digestion with pronase for 5 minutes at room temperature or with 5% trypsin at 37°C for 8–20 minutes depending on antigen. Samples were cooled in distilled water followed by Tris-buffered saline (TBS, 0.05 M) for 2 minutes. Samples were drained and covered with 1–2 drops of Biogenex blocking serum for 30 minutes. Slides were drained and covered with 1–2 drops of primary antibody (rabbit or mouse origin) for 30 minutes or overnight. Sections were rinsed twice in 0.05 M TBS pH 7.4 for 2 minutes. Slides were drained and covered with secondary antibody for 15–30 minutes at room temperature. Slides were rinsed 3 times with 0.05 M TBS pH 7.4 for 2 minutes. Sections were developed in 3,3-diaminobenzidine solution (DAB), prepared by combining 2 ml of Tris, 50 μL of 3% H_2O_2, and 500 μl of stock DAB solution. Sections were developed for 30 seconds to 5 minutes, in parallel with positive controls. Sections were rinsed in TBS and distilled water. Slides were counterstained with Harris hematoxylin for 10–20 seconds, decolorized blue in L_1CO_3, and rinsed in tap water for 1 minute. Sections were dehydrated in 70%, 95%, 100% xylene and cover-slipped using Permount. Appropriate positive and negative controls were used in all cases. Immunohistochemical interpretation was carried out by the authors R. R. Dubielzig, G. Klauss, and M. K. Zarfoss.

The following immunohistochemical stains were performed at the Michigan State University Department of Pathobiology and Diagnostic Investigation: MITF-1, Melan A, S-100, PGP 9.5, laminin. Deparaffinization, antigen retrieval, and counterstaining were performed with an automated immunostainer (Ventana Medical Systems, Inc., Tucson, AZ). Paraffin-embedded tissue sections (5-μm thickness) were deparaffinized with EZ Prep (Ventana Medical Systems, Inc.), washed with Sodium Chloride Sodium Cirrate buffer (SSC) solution (Ventana Medical Systems, Inc.) and incubated with reaction buffer (Ventana Medical Systems, Inc.) at 37°C for 2 minutes. Slides were incubated at 37°C for 10 minutes with a mouse monoclonal anti-MITF-1 (Abcam, Cambridge, UK) and a mouse monoclonal anti-Melan A (DakoCytomation, Carpinteria, CA) at a concentration of 1 : 100 and 1 : 20, respectively. A biotinylated anti-mouse and anti-rabbit secondary antibody conjugated with alkaline phosphatase-streptavidin (enhanced alkaline phosphatase red detection kit, Ventana Medical Systems, Inc.) was applied to locate and visualize the bound primary antibody. After that, sections were incubated at 37°C for 32 minutes, counterstained with hematoxylin, followed with a bluing reagent to change the hue of hematoxylin to blue color (Ventana Medical Systems, Inc.). To remove the liquid cover slip, reagent sections were washed with a detergent and rinsed with warm tap water. Finally, sections were rinsed with 100% ethanol, followed by a 1 : 1 mixture of 50% ethanol and 50% xylene, then 100% xylene, and then cover-slipped. Immunohistochemical staining for PGP 9.5 (R&D Systems, Minneapolis, MN), laminin and S-100 (both Dako Corp.) was performed on a Dako autostainer as previously described[21] with a labeled streptavidin-biotin-peroxidase complex system to visualize the immune reactions. Immunohistochemical positivity was observed and recorded by the authors M. Kiupel and Y. Jones.

The following antibodies were used in immunohistochemical staining at The Ohio State University College of Veterinary Medicine: p53 (Zymed 13-4100, 0.5 mg/ml, detects mutant p53, Zymed Laboratories, Inc., San Francisco, CA), PCNA (Clone PC10, No. M 0879, Dako Corp.), gadd45 (Santa Cruz; C-20, sc-792, Santa Cruz Biotechnology, Inc., Santa Cruz, CA), anti-

Table 1. Signalment, morphology, immunopositivity, and follow-up for 13 uveal spindle-cell tumors of blue-eyed dogs.*

Case No.	Age (in years), Sex, Breed	Antoni A/B	Grade[34]	GFAP	PGP 9.5	Laminin	Gadd45	p53	PCNA
1	10, FS, SH	B	1	+++	++	−	+	−	+
2	10, Unknown sex, Border Collie mix	A/B	1	−	+	−	+	+	−
3	12, MC, SH	A	1	−	++	−	+	−	++
4	4, MC, SH	B	2	+	+	−	−	−	++
5	5, FS, SH	A/B	1	+++					
6	10, FS, SH mix	B	1	+++	−	−	++	+	−
7	10, FS, SH	A/B	2	+	++	+	−	−	++
8	10, MC, SH	A/B	3	+	++	−	+	−	++
9	17, FS, SH	A	3	−					
10	7, MC, SH mix	B	2	−	++	+	+++	+	++
11	5, MC, German Shepherd Dogs	A/B	1	−			++	−	+
12	7, MC, SH	B	2	+					
13	5, MC, Catahoula	B	3	+	−	−			

* GFAP = glial fibrillary acidic protein; PGP 9.5 = protein gene product 9.5; PCNA, proliferating cell nuclear antigen; anti-UVssDNA = antibody for detection of (6-4)-dipyrimidine photoproducts; TERT = telomerase reverse transcriptase; FS = female spayed; SH = Siberian Husky; MC = male castrated; + = 10–25% positive; ++ = 25–50% positive; +++ = >50% positive; − = <10% positive.

UVssDNA (Trevigen Cat No. 4350-MC-100, Trevigen, Inc., Gaithersberg, MD), and TERT (Santa Cruz; L-20, sc7214, Santa Cruz Biotechnology, Inc., Santa Cruz, CA). Protocol for anti-UVssDNA was as follows: 5 μm sections were deparaffinized on slides, incubated in 0.05 N HCl for 5 minutes on ice, and washed 3 times in 1× phosphate-buffered saline (PBS). Slides were incubated in 100 μg/ml RNase in 150 mM NaCl, 15 mM sodium citrate for 1 hour at 37°C, and then washed sequentially in 1× PBS, 50% ethanol, and 70% ethanol for 2 minutes each. DNA was denatured in situ with 0.15 N NaOH in 70% ethanol for 4 minutes at room temperature. Samples were washed sequentially in 70% ethanol, 50% ethanol, and 1× PBS for 2 minutes each, and then incubated in 5 μg/ml proteinase K in 20 mM Tris, 1 mM ethylenediamine tetraacetic acid (EDTA), pH 7.5 for 10 minutes at 37°C. Samples were then washed in 1× PBS. The anti-UVssDNA antibody (primary) was diluted to 6 μg/ml in 1× PBS, 0.01% Tween 20, on ice. Slides were incubated in diluted primary antibody for 1 hour at 37°C (or overnight at 4°C, or at room temperature for 3–4 hours), and then washed 3 times in 1× PBS for 5 minutes each. Slides were incubated in biotinylated anti-mouse antibodies (secondary) for 45 minutes at 37°C, and then washed 10 times in 1× PBS. Slides were incubated in peroxidase-conjugated streptavidin for 30 minutes at 37°C, and then washed 10 times in 1× PBS. Slides were then incubated in Vector NovaRED (chromogen, Vector Laboratories, Burlingame, CA) for 5 minutes at room temperature, and then washed 10 times in tap water. Slides were counterstained in Mayer's hematoxylin counterstain for 3 minutes at room temperature. Slides were then washed 10 times in tap water, dehydrated, mounted, and cover-slipped. Samples were visualized by light microscopy (Olympus BX-50, Olympus America Inc., Center Valley, PA) and digitally photographed (Olympus DP12 digital camera). Positivity was determined by CMHC and KN.

Protocol for PCNA: tissues were deparaffinized, hydrated, and then pretreated with Dako Target Retrieval Solution (catalog No. S1699, Dako Corp.). Retrieval solution was preheated to 90°C. Slides were incubated 20 minutes in steamer, and then cooled for 20 minutes. Slides were placed in Dako wash buffer (TBS/Tween 20, catalog No. S3006, Dako Corp.) for 5 minutes. Procedure on Dako autostainer was as follows: slides were rinsed once with water (rw) × 1, blocked for 5 minutes in peroxidase block in 3% H_2O_2, rw × 1, and rinsed once with wash buffer (rwb) × 1. Slides were then blocked with Dako serum-free protein block (catalog No. X0909, Dako Corp.) for 10 minutes. Samples were subsequently incubated for 30 minutes in primary anti-PCNA antibody, diluted 1 : 200 in Dako antibody diluent with background reducing components (catalog No. S3022, Dako Corp.), rwb × 2. Slides were incubated for 30 minutes in secondary antibody (Vector biotinylated horse anti-mouse, catalog No. BA-2000, diluted 1 : 200, Vector Labs.) in serum-free protein block, rwb × 2 and placed for 30 minutes in ABC (Vector R.T.U. Vectastain elite ABC, catalog No. PK-7100, Vector Labs.), rwb × 2, rw × 1, incubated for 5 minutes in Dako liquid DAB substrate (catalog No. K3466, Dako Corp.), rw × 1, rwb × 1. Slides were counterstained for 2 minutes in Richard-Allen hematoxylin 2 (Richard-Allen Scientific, Kalamazoo, MI) catalog No. 7231, rw × 2, dehydrated, and cover-slipped.

Table 1. Extended.

Anti-UVssDNA	TERT	Follow-up: Tumor-free Duration (in months), Suspected Reason for Death (if known)
−	+	23, Euthanasia due to arthritis
−	+	12, Liver/thoracic tumor suspected at death
−	−	24
++	+	13
		24
−	+++	28, Epistaxis, but no evidence of orbital disease at death
+	+	Lost to follow-up
+	+	9, Euthanized with splenic mass
		8, Died with seizures
+	−	Lost to follow-up
+	−	12
		28, Euthanized, posterior paresis
		10

Protocol for TERT (1 : 350), p53, gadd45 (1 : 250) was as follows: samples were deparaffinized, rehydrated, and blocked with 3% peroxidase for 10 minutes at 37°C. Power Block (1×, catalog No. BS-1310-25, Biogenex, San Ramon, CA) was used for 10 minutes at 37°C. The sample was incubated with primary antibody for 1 hour at 37°C, and then washed. The sample was incubated in secondary antibody (super-sensitive label, peroxidase-conjugated streptavidin) for 30 minutes at 37°C, and then washed. Positivity was detected using Vector NovaRED for 5 minutes before washing. Samples were counterstained with Mayer's hematoxylin for 3 minutes at room temperature, washed, dehydrated, and coverslipped. Positive controls for gadd45 and TERT were cataractous lens epithelial cells.[8] Negative controls, where primary of secondary antibodies were omitted, were performed in all cases.

For electron microscopy, 1 mm^3 of 2 formalin-fixed tumors were harvested and postfixed in gluteraldehyde. This tissue was postfixed a second time in osmium tetroxide and embedded in acrylic resin. Thin sections (approximately 90 nm) were cut, mounted on 200-mesh copper grids, stained with 5% methanolic uranyl acetate and Reynolds' lead citrate, and examined and photographed on a Philips 410 transmission electron microscope (Philips Medical Systems, Andover, MA).

Results

For signalment, follow-up, morphologic characteristics, and immunohistochemical results, see Table 1. While there was no sex predilection, Siberian Husky purebred or mix dogs were overrepresented (10/13 cases). The median age was 10 years. Histologically, all tumors asymmetrically expanded the iris and ciliary body and consisted entirely of spindle-shaped mesenchymal cells (Figs. 1–4). Tumor cells formed solid sheets of interwoven bundles, streams or whorls, often with palisading nuclei. Tumor morphology, nuclear features, necrosis, and mitotic index were highly variable. Antoni A and/or Antoni B behavior were exhibited by all tumors, consistent with human schwannomas (Figs. 3, 4).[32] Tumors were graded as 1, 2, or 3 as previously described.[34] All cases exhibited some degree of lymphoplasmacytic uveitis. Most cases (except for cases 2, 4, 11, and 13) exhibited either clinical or histopathologic evidence of glaucoma (historical ocular hypertension, loss of retinal ganglion cells, optic nerve cupping/gliosis). Other secondary findings within the globes included preiridal fibrovascular membranes, intraocular hemorrhage, peripheral corneal stromal neovascularization and inflammatory infiltrate, and cataract.

All dogs tested were negative for SMA (6/6), desmin (6/6), Melan A (7/7), and MITF-1 (7/7) and positive for vimentin (10/10) and S-100 (7/7). The tumors were positive for GFAP in 9/13 dogs, positive for PGP 9.5 in 7/9 dogs, and positive for laminin in 2/9 dogs (Figs. 5–7). Results for gadd45, p53, PCNA, anti-UVssDNA, and TERT were variable and are shown in Table 1 and Figs. 8–10.

Follow-up ranged from 0–28 months (see Table 1). While several patients died with clinical signs consistent with thoracic and abdominal metastasis, no necropsies were performed. Furthermore, dogs with possible metastases did not have any obvious morphologic or immunohistochemical similarities that might relate to prognosis.

Electron microscopic findings revealed that tumor cells had long interdigitating cytoplasmic processes and intermittent basal laminae at the plasma membrane (Fig. 11). The extracellular matrix consisted of collagen bundles.

Discussion

Immunohistochemical stains were initially performed to rule out nonneural tumors. Vimentin immunoreactivity suggests that this tumor is of mesenchymal origin.[13] Leiomyosarcoma or rhabdomyosarcoma are unlikely because the tumors did not stain for SMA and desmin.[5] MITF-1 and Melan A immunonegativity suggest that this tumor is not of melanocyte origin.[6,16] Immunohistochemical staining for c-kit was also performed on nine tumors (CD117, results not shown); all tumor cells were immunonegative. The GFAP immunopositivity makes a diagnosis of fibrosarcoma unlikely.[38]

Glial fibrillary acidic protein staining, in 9/13 dogs, suggests central nervous system/astrocyte

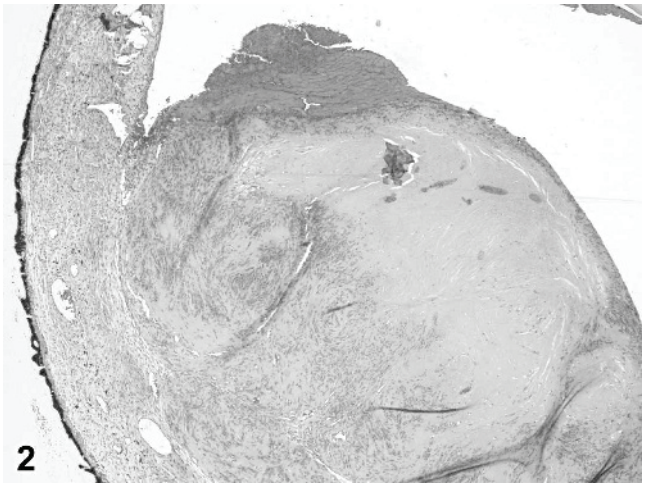

Fig. 2. Iris; dog No. 3. Along the left, relatively normal iris stroma is bordered by posterior iridal epithelium. To the right, there is a round mass of mesenchymal cells lined anteriorly by hemorrhage. Within the center of the image, the neoplastic cells exhibit Antoni A behavior. HE stain.

origin; however, GFAP positivity has also been associated with both nonmyelinating Schwann cells[52] and normal rodent uvea.[4] Electron microscopy was also consistent with a tumor of peripheral nerve sheath origin due to the interrupted basal laminae between cells.[32] Protein gene product 9.5 is a relatively neuron-specific protein similar to neuron-specific enolase.[51] Laminin is found in basement membranes of endothelial cells, smooth muscle cells, and Schwann cells.[5] Laminin staining was positive in only 2/9 cases. Formalin fixation may have interfered with stain uptake, or laminin expression may have been variable. This tumor is immunohistochemically and morphologically most consistent with a peripheral nerve sheath tumor, which arises from Schwann cells, neurofibroblasts, or other perineural cells.[32] Such tumors in animals are generally classified as (benign) schwannomas or malignant peripheral nerve sheath tumors. The presence of Antoni A and B patterns in these tumors is also consistent with neural origin.[26,32]

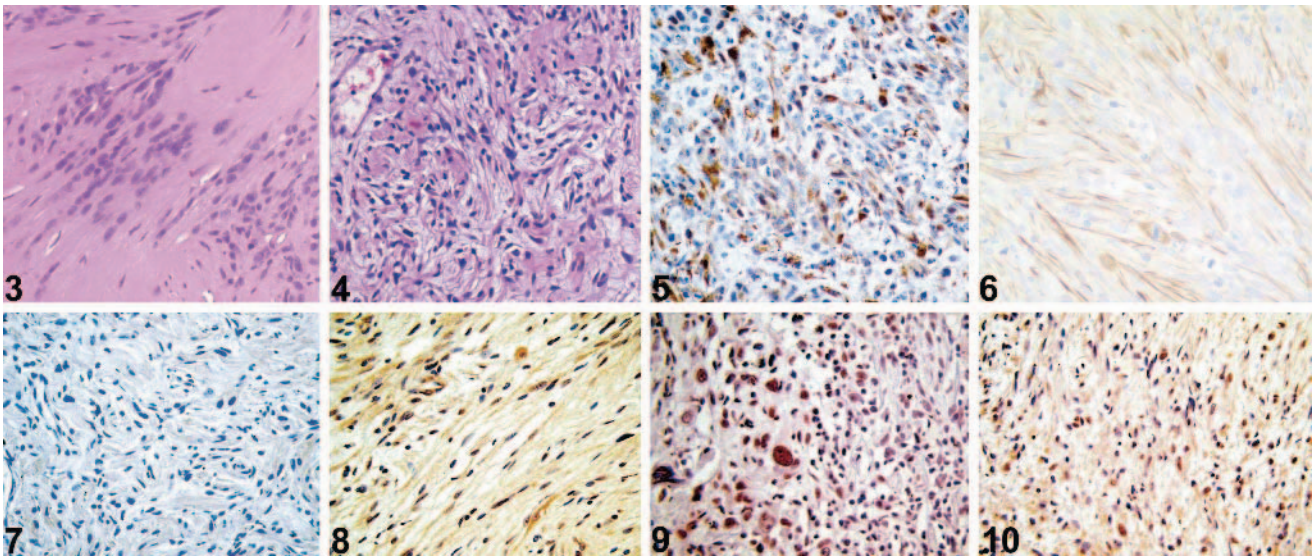

Fig. 3. Uveal spindle-cell tumor; dog No. 3. Antoni A behavior is shown. HE stain.
Fig. 4. Uveal spindle-cell tumor; dog No. 1. Antoni B behavior is shown. HE stain.
Fig. 5. Uveal spindle-cell tumor; dog No. 8. Intracytoplasmic immunopositivity is shown. S-100 immunohistochemistry.
Fig. 6. Uveal spindle-cell tumor; dog No. 13. Intracytoplasmic immunopositivity is shown. Glial fibrillary acidic protein (GFAP) immunohistochemistry.
Fig. 7. Uveal spindle-cell tumor; dog No. 7. Extracellular immunopositivity is shown. Laminin immunohistochemistry.
Fig. 8. Uveal spindle-cell tumor; dog No. 11. Nuclear and cytoplasmic immunopositivity is shown. Growth arrest and DNA damage45 (Gadd45) immunohistochemistry.
Fig. 9. Uveal spindle-cell tumor; dog No. 8. Nuclear immunopositivity is shown. UV single strand DNA (UVssDNA) immunohistochemistry.
Fig. 10. Uveal spindle-cell tumor; dog No. 6. Nuclear and cytoplasmic immunopositivity is shown. Telomerase reverse transcriptase (TERT) immunohistochemistry.

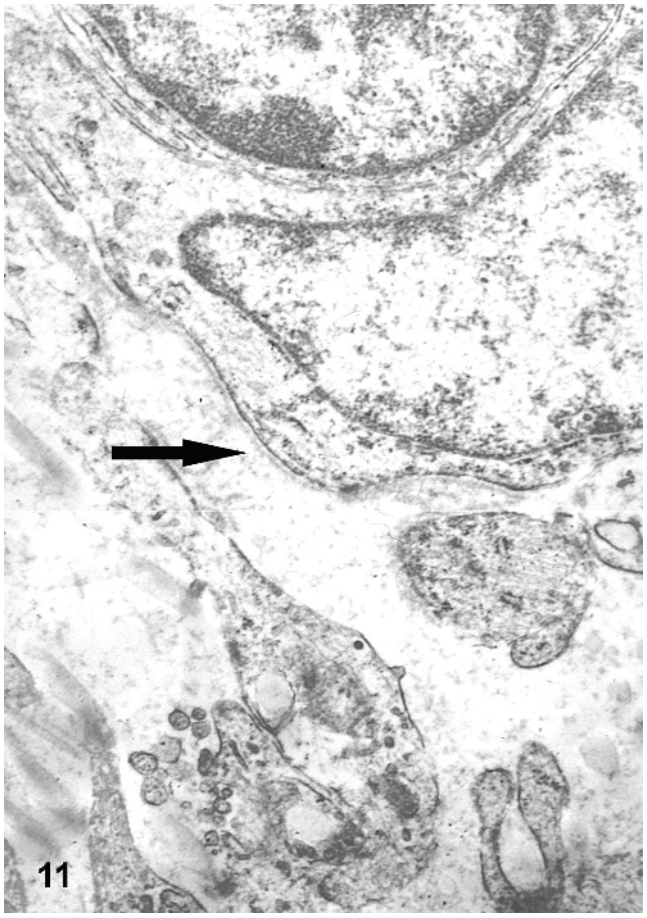

Fig. 11. Electron microscopic image of spindle-cell tumor; dog No. 10. The arrow is directed at the basal lamina.

While electron microscopy, light microscopy, and GFAP immunohistochemistry are most consistent with a schwannoma, these findings cannot reliably differentiate between a benign/malignant schwannoma, neurofibroma, neurofibrosarcoma, or other tumor of nerve origin in dogs.[25,52]

To the authors' knowledge, no intraocular peripheral nerve sheath tumors have been reported in the dog except for a recent case report by Sato et al.[43] While morphologically similar to the tumors in this study, those authors clearly stated in a personal correspondence (Sato) that there were no identifiably blue areas in the affected (or unaffected) eye of their patient, a Shetland Sheepdog. This tumor immunohistochemically stained positively for S-100 and vimentin. At the COPLOW, no similar uveal tumors have been diagnosed in any other species or in brown-eyed dogs. Relative to brown-eyed dogs, blue-eyed dogs are at much higher risk for this tumor. Other studies have shown extraocular, benign, canine schwannomas to be vimentin positive (most consistent feature), desmin negative, variably GFAP positive, and often S-100 positive.[32,38]

Why do these tumors only occur in dogs with blue irides? To answer this question, the embryology and anatomy of the canine iris must be considered. While recent studies suggest that mammalian uveal stroma is formed from a mixture of neural crest and mesoderm, neural crest is believed to give rise to melanocytes within the iris.[10,15,24] The color of the iris is normally dictated by heritable factors and determined by the pigment granules within the posterior iris epithelium, Rayleigh scattering of light by the stromal extracellular matrix, type of melanin, and the number and area of melanin granules within the iris stromal melanocytes.[24,50] Aside from polygenic inheritance affecting melanin content of the iris, blue iridal color can result from a tyrosinase defect preventing melanin production in stromal melanocytes (heterochromic laboratory beagles,[45] albinism, Siamese cats[48]), as well as abnormal neural crest migration into the uvea causing an absence of stromal melanocytes (white cats, associated with deafness[3]). At the COPLOW, two goniodysgenic canine irides (lacking tumor) were stained with GFAP. These irides showed increased linear GFAP positivity, consistent with nonmyelinated nerves, within the iris stroma compared with a similarly stained, bleached brown iris. Melan A immunohistochemistry on the same 2 goniodysgenic canine blue eyes found no convincingly positive melanocytes within the iridal stroma (results not shown). Lack of melanocytes within the uveal stroma would corroborate that this is not a primary intraocular melanocytic tumor; furthermore, it suggests a defect in neural crest. However, these findings cannot necessarily be extrapolated to *all* blue-eyed dogs; furthermore, the coat color of the patients with uveal spindle cell tumors was generally not recorded.

In addition to iridal melanocytes, neural crest is also responsible for the development of peripheral nerve tissue, including Schwann cells.[35] In human neural crest–related diseases, genetic mutations in PAX 3 gene (Waardenburg syndrome) and NF1 gene (neurofibromatosis) are associated with hypopigmented irides or light brown iridal café au lait spots, respectively.[23,42] While iris color is not necessarily blue in humans with neurofibromatosis, iridal lesions include pigmented hamartomas that are considered to be of neural crest origin (Lisch nodules).[23] The NF1 gene is a tumor suppressor gene and neurofibromas and schwannomas are a feature of neurofibromatosis. Peripheral nerve sheath tumors related to human neurofibromatosis 1 are usually benign but can undergo malignant

transformation.[14,37] More research needs to be performed to determine whether or not a genetic defect in neural crest development contributes to oncogenesis in this tumor (particularly in Siberian Huskies).[7]

Ultraviolet radiation has been shown to contribute to oncogenesis in many tumors, including uveal melanoma.[20,22,44,46] Schwannomas have been reported in humans in association with radiation therapy (but not UV damage).[41] Positive immunohistochemical staining for p53, anti-UVssDNA, PCNA, gadd45, and TERT have all been associated with UV damage and oncogenesis. Specifically, research suggests that gadd45 and PCNA facilitate repair after DNA undergoes UV-related damage.[1,47] Telomerase refers to a ribonucleoprotein complex that has 2 main components: an RNA subunit (TR) and a catalytic subunit (TERT). All cells express TR, but TERT is only expressed in cells that have telomerase activity. Telomerase activity facilitates repeated cell division and is therefore necessary for tumor proliferation.[17,18] Up-regulation of TERT is strongly associated with exposure to the sun in normal human skin samples and exposure to UV radiation results in increased telomerase activity in lens epithelial cells, cultured splenocytes, and fibroblasts, suggesting a role in UV-induced oxidative stress.[9,18,19,49] In one study, 100% of tumor samples with UV-specific p53 mutations also exhibited TERT activity; both telomerase activity and p53 mutations have been implicated in oncogenesis.[49] The p53 gene is commonly mutated in human cancers and is integral in DNA repair after UV damage;[47] it controls cell cycle arrest, apoptosis, and senescence, among other antitumor functions.[12] Mutations in p53 cause increased p53 expression because the mutated form has a much longer half-life than the wild-type form.[27] The UVssDNA antibody is specific for proteins that contain the (6-4)-dipyrimidine photoproduct, a product of UV damage.[53] With this in mind, increased expression of gadd45, PCNA, TERT, p53, and anti-UVssDNA should all be up-regulated in tumors influenced by UV damage.

The results of this study were inconsistent for markers of UV-induced tissue damage and do not clearly support a role for UV damage in the development of this tumor. However, these results do not exclude UV damage as a factor because UV markers are in some cases only temporarily up-regulated after UV damage.[36] There are other unmeasured effects of UV radiation[36] and other UV-related antibodies that were not available for use in this study.[31] Technically, inconsistent immunohistochemical results may be due to (delayed) fixation,[13,52] anaplasia, or multiple cellular origins. Uveal spindle-cell tumors of blue-eyed dogs may arise as a result of a multifactorial process including a genetic neural crest defect *and* UV damage.[40] Other melanin-related or genetic mechanisms may also be in play. Melanin has been shown to be associated with intraocular zinc storage (an antioxidant).[33]

We present 13 cases of a uveal spindle-cell tumor of blue-eyed dogs with morphologic and immunohistochemical features most consistent with a schwannoma. Morphologic features of malignancy were variable. While several of the dogs have died with clinical signs consistent with metastatic disease, no necropsies have been performed. The cell of origin, its relationship to neural crest, and the contribution of UV damage in the pathogenesis of uveal tumors in blue-eyed dogs have yet to be fully elucidated. Until that time, we will continue to refer to these tumors as uveal spindle-cell tumors of blue-eyed dogs. These tumors continue to accumulate at the COPLOW. We will continue to examine these cases and seek follow-up to better assess their behavioral malignancy. This tumor should be considered as a differential diagnosis in all intraocular masses arising in the blue canine uvea.

Acknowledgements

The authors would like to thank Drs. Steven Weisbrode and Donna Kusewitt for expert consultation. The authors would also like to thank the referring veterinarians and owners of these dogs for providing follow-up information.

References

1 Aboussekhra A, Wood RD: Detection of nucleotide excision repair incisions in human fibroblasts by immunostaining for PCNA. Exp Cell Res **221:** 326–332, 1995

2 Agar N, Young AR: Melanogenesis: a photoprotective response to DNA damage? Mutat Res **571:** 121–132, 2005

3 Bergsma DR, Brown KS: White fur, blue eyes, and deafness in the domestic cat. J Hered **62:**171–185, 1971

4 Bjorklund H, Dahl D: Glial fibrillary acidic protein (GFAP)-like immunoreactivity in the rodent eye. J Neuroimmunol **8:**331–345, 1985

5 Cerilli LA, Wick MR: Immunohistology of soft tissue and osseus neoplasms. *In:* Diagnostic Immunohistochemistry, ed. Dabbs DJ, pp. 59–112. Churchill Livingston, New York, NY, 2002

6 Choi C, Kusewitt DF: Comparison of tyrosinase-related protein-2, S-100, and Melan A immunoreac-

tivity in canine amelanotic melanomas. Vet Pathol **40:**713–718, 2003
7 Clark LA, Wahl JM, Rees CA, Murphy KE: Retrotransposon insertion in SILV is responsible for merle patterning of the domestic dog. Proc Natl Acad Sci USA **103:**1376–1381, 2006
8 Colitz CM, Davidson MG, McGahan MC: Telomerase activity in lens epithelial cells of normal and cataractous lenses. Exp Eye Res **69:**641–649, 1999
9 Colitz CM, Whittington A, Carter R, Warren J: The effects of oxidative stress on telomerase activity and other stress-related proteins in lens epithelial cells. Exp Eye Res **78:**235–242, 2004
10 Creuzet S, Vincent C, Couly G: Neural crest derivatives in ocular and periocular structures. Int J Dev Biol **49:**161–171, 2005
11 Diters RW, Dubielzig RR, Aguirre GD, Acland GM: Primary ocular melanoma in dogs. Vet Pathol **20:**379–395, 1983
12 el-Deiry WS: Regulation of p53 downstream genes. Semin Cancer Biol **8:**345–357, 1998
13 Elias JM: Immunohistopathology: A Practical Approach to Diagnosis, ASCP Press, Chicago, IL, 1990
14 Ferner RE, O'Doherty MJ: Neurofibroma and schwannoma. Curr Opin Neurol **15:**679–684, 2002
15 Gage PJ, Rhoades W, Prucka SK, Hjalt T: Fate maps of neural crest and mesoderm in the mammalian eye. Invest Ophthalmol Vis Sci **46:**4200–4208, 2005
16 Goding CR: Mitf from neural crest to melanoma: signal transduction and transcription in the melanocyte lineage. Genes Dev **14:**1712–1728, 2000
17 Greider CW: Telomerase activity, cell proliferation, and cancer. Proc Natl Acad Sci USA **95:**90–92, 1998
18 Hande MP, Balajee AS, Natarajan AT: Induction of telomerase activity by UV-irradiation in Chinese hamster cells. Oncogene **15:**1747–1752, 1997
19 Hande MP, Lansdorp PM, Natarajan AT: Induction of telomerase activity by in vivo X-irradiation of mouse splenocytes and its possible role in chromosome healing. Mutat Res **404:**205–214, 1998
20 Harbour JW, Brantley MA Jr, Hollingsworth H, Gordon M: Association between choroidal pigmentation and posterior uveal melanoma in a white population. Br J Ophthalmol **88:**39–43, 2004
21 Hoenerhoff MJ, Kiupel M, Rosenstein D, Pool RR: Multipotential osteosarcoma with various mesenchymal differentiations in a young dog. Vet Pathol **41:**264–268, 2004
22 Hu DN: Photobiology of ocular melanocytes and melanoma. Photochem Photobiol **81:**506–509, 2005
23 Huson S, Jones D, Beck L: Ophthalmic manifestations of neurofibromatosis. Br J Ophthalmol **71:**235–238, 1987
24 Imesch PD, Bindley CD, Khademian Z, Ladd B, Gangnon R, Albert DM, Wallow IH: Melanocytes and iris color: electron microscopic findings. Arch Ophthalmol **114:**443–447, 1996
25 Kennedy PGE: Neural cell markers and their applications to neurology. J Neuroimmunol **2:**35–53, 1982
26 Kim IT, Chang SD: Ciliary body schwannoma. Acta Ophthalmol Scand **77:**462–466, 1999
27 Kindblom L-G, Ahlden M, Meis-Kindblom JM, Stenman G: Immunohistochemical and molecular analysis of p53, MDM2, proliferating cell antigen and Ki67 in benign and malignant peripheral nerve sheath tumours. Virchows Arch **427:**19–26, 1995
28 Klauss G, Dubielzig R: Characteristics of primary spindle cell neoplasms of the anterior uveal tract in eleven dogs. American College of Veterinary Pathologists Annual Conference. Vet Pathol **38:**574, 2001
29 Klauss G, Dubielzig R: Primary spindle cell neoplasms of the anterior uveal tract of fourteen dogs. American College of Veterinary Ophthalmologists Annual Conference, 2001 p 55.
30 Kliman GH, Augsburger JJ, Shields JA: Association between iris color and iris melanocytic lesions. Am J Ophthalmol **100:**547–548, 1985
31 Kobayashi N, Katsumi S, Imoto K, Nakagawa A, Miyagawa S, Furumura M, Mori T: Quantitation and visualization of ultraviolet-induced DNA damage using specific antibodies: application to pigment cell biology. Pigment Cell Res **14:**94–102, 2001
32 Koestner A, Higgins RJ: Tumors of the nervous system. *In:* Tumors in Domestic Animals, ed. Meuten DJ, pp. 697–738. Iowa State Press, Ames, IA, 2002
33 Kokkinou D, Kasper HU, Bartz-Schmidt KU, Schraermeyer U: The pigmentation of human iris influences the uptake and storing of zinc. Pigment Cell Res **17:**515–518, 2004
34 Kuntz CA, Dernell WS, Powers BE, Devitt C, Straw RC, Withrow SJ: Prognostic factors for surgical treatment of soft-tissue sarcomas in dogs: 75 cases (1986–1996). J Am Vet Med Assoc **211:**1147–1151, 1997
35 Larsen WJ: Human Embryology. Churchill Livingstone, Philadelphia, PA, 2001
36 Matsumura Y, Anathaswamy HN: Toxic effects of ultraviolet radiation on the skin. Toxicol Appl Pharmacol **195:**298–308, 2004
37 Murovic JA, Kim DH, Kline DG: Neurofibromatosis-associated nerve sheath tumors: case report and review of the literature. Neurosurg Focus **20:**E1, 2006
38 Perez J, Bautista MJ, Rollon E, de Lara FC, Carrasco L, Martin de las Mulas J: Immunohistochemical characterization of hemangiopericytomas and other spindle cell tumors in the dog. Vet Pathol **33:**391–397, 1996
39 Pfeifer GP, You YH, Besaratinia A: Mutations induced by ultraviolet light. Mutat Res **571:**19–31, 2005
40 Robanus-Maandag E, Giovannini M, va der Valk M, Niwa-Kawakita M, Abramowski V, Antonescu C, Thomas G, Berns A: Synergy of Nf2 and p53 mutations in development of malignant tumours of neural crest origin. Oncogene **23:**6541–6547, 2004

41 Rubinstein AB, Reichenthal E, Borohov H: Radiation-induced schwannomas. Neurosurgery **24:**929–932, 1989
42 Sarnat HB, Flores-Sarnat L: Embryology of the neural crest: its inductive role in the neurocutaneous syndromes. J Child Neurol **20:**637–643, 2005
43 Sato T, Yamamoto A, Shibuya H, Sudo H, Shirai W, Amemori T: Intraocular peripheral nerve sheath tumor in a dog. Vet Ophthalmol **8:**283–286, 2005
44 Shah CP, Weis E, Lajous M, Shields JA, Shields CL: Intermittent and chronic ultraviolet light exposure and uveal melanoma: a meta-analysis. Ophthalmology **112:**1599–1607, 2005
45 Shively JN, Phemister RD: Fine structure of the iris of dogs manifesting heterochromia iridis. Am J Ophthalmol **66:**1152–1162, 1968
46 Singh AD, Rennie IG, Seregard S, Giblin M, McKenzie J: Sunlight exposure and pathogenesis of uveal melanoma. Surv Ophthalmol **49:**419–428, 2004
47 Smith ML, Ford JM, Hollander MC, Bortnick RA, Amundson SA, Seo YR, Deng CX, Hanawalt PC, Fornace AJ Jr: p53-mediated DNA repair responses to UV radiation: studies of mouse cells lacking p53, p21, and/or gadd45 genes. Mol Cell Biol **20:**3705–3714, 2000
48 Thibos LN, Levick WR, Morstyn R: Ocular pigmentation in white and Siamese cats. Invest Ophthalmol Vis Sci **19:**475–486, 1980
49 Ueda M, Ouhtit A, Bito T, Nakazawa K, Lubbe J, Ichihashi M, Yamasaki H, Nakazawa H: Evidence for UV-associated activation of telomerase in human skin. Cancer Res **57:**370–374, 1997
50 Wilkerson CL, Syed NA, Fisher MR, Robinson NL, Wallow IH, Albert DM: Melanocytes and iris color: light microscopic findings. Arch Ophthalmol **114:**437–442, 1996
51 Wilkinson KD, Lee K, Deshpande S, Duerksen-Hughes P, Boss JM, Pohl J: The neuron-specific protein PGP 9.5 is a ubiquitin carboxyl-terminal hydrolase. Science **246:**670–673, 1989
52 Yen S-H, Fields KL: A protein related to glial filaments in Schwann cells. Ann N Y Acad Sci **455:**538–551, 1985
53 Zavala AG, Lancaster T, Groopman JD, Strickland PT, Chandrasegaran S: Phage display of ScFv peptides recognizing the thymidine(6-4)thymidine photoproduct. Nucleic Acids Res **28:**E24, 2000

Request reprints from R. R. Dubielzig, University of Wisconsin-Madison, Department of Pathobiological Sciences, 2015 Linden Drive, Madison, WI 53706 (USA). E-mail: dubielzr@svm.vetmed.wisc.edu.